Table VI. Dipole Moments

Compound	Predicted dipole moment, D.	Exptl dipole moment, D.
cis-1,2-Dimethylcyclopropane (II)	0.15	
trans-1,2-Dimethylcyclopropane (III)	0.01	
Bicyclo[1.1.0]butane (IV)	0.35	0.68[a]
1,3-Dimethylbicyclo[1.1.0]butane (V)	0.34	
Methylenecyclopropane (VII)	0.18	
exo-Methylmethylenecyclopropene (VIII)	0.26	
2-Methylmethylenecyclopropane (IX)	0.18	
Dimethylenecyclopropane (X)	0.12	
Cyclopropene (XII)	0.27	0.45[b]
1-Methylcyclopropene (XIII)	0.41	
1,2-Dimethylcyclopropene (XIV)	0.45	
Methylenecyclopropene (XV)	0.87	
3-Methylcyclopropene (XIX)	0.34	

[a] M. D. Harmony and K. Cox, *J. Am. Chem. Soc.*, **88**, 5049 (1966). [b] P. H. Kasai, R. J. Meyers, D. F. Eggers, Jr., and K. B. Wiberg, *J. Chem. Phys.*, **30**, 512 (1959).

Table VII. Energy Levels (ev)

I	11.08, 13.16, 13.71, 15.85, 19.77
II	10.82, 10.85, 12.03, 12.45, 12.93, 13.24, 14.09, 14.17, 14.90, 15.83, 17.84, 19.32
III	10.80, 10.88, 12.07, 12.63, 13.15, 13.79, 14.09, 14.26, 14.46, 15.05, 18.61, 19.04
IV	10.39, 10.87, 11.67, 11.96, 13.60, 14.00, 15.45, 18.35, 18.79
V	10.21, 10.77, 11.03, 11.89, 12.54, 13.65, 13.75, 13.95, 14.33, 14.63, 15.21, 16.39, 17.78
VI	9.58, 11.72, 14.90, 18.68
VII	10.74, 10.81, 10.94, 13.03, 13.30, 14.46, 15.29, 17.13, 19.53
VIII	10.61, 10.69, 10.92, 13.03, 13.21, 14.26, 14.50, 15.31, 16.87, 19.51
IX	10.67, 10.76, 10.81, 12.39, 13.09, 13.80, 14.12, 14.48, 15.02, 17.02, 18.84
X	10.19, 10.57, 10.87, 11.27, 13.16, 14.20, 14.51, 14.61, 16.02, 18.17
XI	10.21, 10.57, 12.58, 13.06, 14.13, 14.42, 16.21
XII	10.32, 10.86, 11.38, 14.40, 14.42, 18.34, 19.66
XIII	10.18, 10.62, 11.13, 13.50, 14.02, 14.33, 14.66, 16.92, 19.42
XIV	10.06, 10.45, 10.88, 12.91, 13.95, 14.15, 14.18, 14.40, 14.80, 15.73, 18.68
XV	9.60, 10.69, 11.49, 12.28, 14.03, 14.06, 17.09, 18.64
XVIa	9.16, 11.09, 11.64, 12.51, 13.02, 16.73, 16.83
XVII	10.64, 10.68, 11.87, 13.12, 13.28, 13.76, 15.23, 17.13, 19.84
XVIII	9.58, 10.92, 12.10, 12.68, 14.76, 17.42, 18.44
XIX	10.24, 10.73, 11.28, 13.07, 13.65, 14.09, 14.88, 18.42, 18.55

In part I[1] it was shown that there is a remarkable correlation between the orbital energies calculated by our method and the ionization potentials measured by Al-Jaboury and Turner[17] by their novel photoelectron spectroscopic technique. The correlation held for all orbitals with binding energies up to 20 ev. No good data seem as yet to be available for any of the compounds discussed in this paper; the few values reported were obtained by electron impact and therefore both are numerically unreliable and also refer only to the first ionization potentials.[17] Undoubtedly photoelectron spectroscopic studies will soon become available for these materials; we have therefore listed our calculated orbital energies in Table VII, in the hope that they may assist in interpreting such measurements.

(17) M. I. Al-Jaboury and D. W. Turner, *J. Chem. Soc.*, 5141 (1963); 4434 (1964); 616 (1965).

Nuclear Magnetic Resonance Studies on Exchange Reactions of Group III Alkyl Derivatives. II

J. Barry DeRoos[1] and John P. Oliver

Contribution from Wayne State University, Detroit, Michigan 48202.
Received August 8, 1966

Abstract: The exchange of trimethylgallium with trimethylgallium–dimethylamine (I), trimethylgallium–monomethylamine (II), trimethylgallium–ammonia (III), and trimethylgallium–dimethyl ether (IV) addition compounds has been investigated. This exchange proceeds through a dissociation step for I, but has been shown to proceed by an electrophilic displacement reaction for II and III. Activation energies were determined to be 19, 10, and 8.5 kcal/mole, respectively, for I, II, and III. The reaction of IV was too fast to follow by the techniques available. An explanation for this drastic change in mechanism is given, and the results are compared with those observed for similar exchange reactions of boron trifluoride addition compounds.

There has been a rapidly expanding interest in the exchange reactions of group III addition compounds as cited previously.[2] Unfortunately, there is still considerable confusion regarding the mechanisms of molecular exchange in these systems. Brownstein, *et al.*,[3] present two possible mechanisms for exchange in BF_3–base systems: dissociation

$$AB \underset{k_2}{\overset{k_1}{\rightleftharpoons}} A + B \quad (1)$$

or bimolecular displacement

$$A' + AB \overset{k_1}{\rightleftharpoons} A'B + A \quad (2)$$

Their data suggest that both mechanisms may be operative depending upon the base present, but it is difficult to establish any trends for the reported reactions be-

(1) Recipient of a NASA Traineeship for 1964–1966.
(2) J. B. DeRoos and J. P. Oliver, *Inorg. Chem.*, 4, 1741 (1965).
(3) S. Brownstein, A. M. Eastham, and G. A. Latremouille, *J. Phys. Chem.*, 67, 2020 (1963); S. Brownstein and J. Paasivirta, *J. Am. Chem. Soc.*, 87, 3593 (1965).

cause insufficient data are given to fully evaluate mechanism 2.[3]

Rutenberg, *et al.*,[4] have examined systems which contain BF_3 in the presence of two or more ethers, thus complicating the exchange by the presence of two complex species and offering an additional pathway for exchange.

$$AB + A'B' \overset{k}{\rightleftharpoons} AB' + A'B \qquad (3)$$

Furthermore, they suggest that several competing reactions are necessary to explain the variations which were observed for the activation energy of the different reactions but only consider mechanisms for exchange by paths 2 and 3, ruling out the dissociation mechanisms because of the low activation energies obtained. Recently we reported a mechanism for the molecular exchange reaction in the $(CH_3)_3Ga$–$N(CH_3)_3$ system, which shows that the exchange of $(CH_3)_3Ga$ goes by the dissociation process 1 in the presence of $(CH_3)_3Ga$.[2] In this paper the kinetics for the exchange reactions in $(CH_3)_3Ga$–$N(CH_3)_2H$, $(CH_3)_3Ga$–$N(CH_3)H_2$, $(CH_3)_3Ga$–NH_3, and $(CH_3)_3Ga$–$O(CH_3)_2$ systems are reported. The mechanisms of exchange in the above systems show an abrupt change from a dissociation process (eq 1) to an electrophilic displacement (eq 2) with no evidence for exchange taking place through the process described by eq 3.

Experimental Section

Trimethylgallium was prepared and purified as described previously[2] and then stored at −78° to prevent decomposition. Dimethylamine, monomethylamine, ammonia, and dimethyl ether were obtained from the Matheson Co., anhydrous, and were used as obtained. Deuteration of the N–H protons on dimethylamine was accomplished by the following reactions.

$$C_4H_9Li + (CH_3)_2NH \longrightarrow C_4H_{10} + LiN(CH_3)_2$$
$$LiN(CH_3)_2 + D_2O \longrightarrow LiOD + (CH_3)_2ND$$

Isotopic purity was checked by integration of the nmr resonance of the N–H protons and found to be better than 99% N–D.

The $N–H_2$ protons on monomethylamine were deuterated by exchange with D_2O. Isotopic purity, checked by the same procedure as above, showed 96% $N–D_2$.

Freon 11, used as a solvent in all samples, was obtained from E. I. du Pont de Nemours and Co., dried over magnesium perchlorate, and distilled before use.

Samples were prepared by pressure measurement in a calibrated volume followed by direct condensation into an nmr tube. A measured volume of solvent was added before sealing the sample under vacuum.

The nmr spectra were run on a Varian Associates A-60A spectrometer equipped with a variable-temperature probe. Temperature control in the probe was approximately ±1° after the sample had equilibrated for 15 min.

A program was written for an IBM 7074 computer to calculate theoretical line shapes for exchange between two magnetically nonequivalent sites. Both lifetime and concentration were used as variables so that line shapes could be calculated for all cases encountered. This program was then used to estimate lifetimes from spectra where conditions for slow exchange were not met or where good estimates of the line width could not be obtained. The nonexchange line widths were obtained from low-temperature spectra and from spectra of the pure materials. This was found to lie between 0.5 and 0.6 cps in all cases, and the value 0.55 cps was used in all later calculations.

Results

In a previous paper[2] we reported that the exchange of $(CH_3)_3GaN(CH_3)_3$ with excess $(CH_3)_3Ga$ proceeds through a dissociation mechanism with an activation energy of 23 kcal/mole. This investigation has now been extended to the following systems, $(CH_3)_3Ga$–$N(CH_3)_2H$, $(CH_3)_3Ga$–$N(CH_3)H_2$, $(CH_3)_3Ga$–NH_3, and $(CH_3)_3Ga$–$O(CH_3)_2$, where the quantitative kinetic data were obtained by nmr line-broadening techniques over the widest possible temperature range where the conditions of slow exchange apply (*i.e.*, $\tau \gg (\omega_A - \omega_B)^{-1}$.

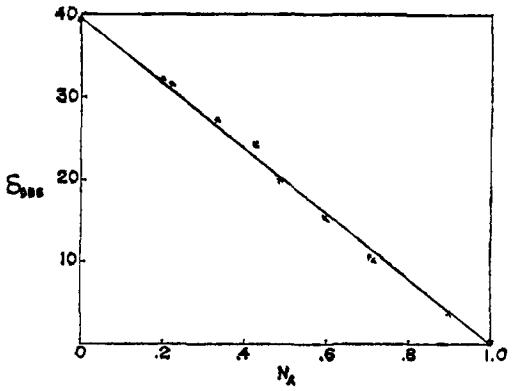

Figure 1. The observed chemical shift of $(CH_3)_3Ga$ protons *vs.* mole fraction of free $(CH_3)_3Ga$ in the $(CH_3)_3Ga$–$N(CH_3)_2H$ system calculated assuming all possible adduct is formed at +36°.

The $(CH_3)_3Ga$–$N(CH_3)_2H$ Systems. One obtains proof for rapid chemical exchange of $(CH_3)_3Ga$ at 36° by the linear dependence of the chemical shift of the observed single resonance line on the mole fractions of $(CH_3)_3Ga$ calculated assuming all possible adduct is formed as shown in Figure 1. The concentration dependence of the lifetimes of $(CH_3)_3Ga$ (τ_A) and $(CH_3)_3GaN(CH_3)_2H$ (τ_{AB}) were studied at +11° where the conditions of slow exchange are met. Table I shows that the lifetime of $(CH_3)_3GaN(CH_3)_2H$ is virtually independent of concentration, while the lifetime of $(CH_3)_3Ga$ is obviously concentration dependent.

Table I. Concentration Dependence for the Lifetimes of $(CH_3)_3GaN(CH_3)_2H$ (τ_{AB}) and $(CH_3)_3Ga$ (τ_A) at +11°

C_{AB}, M	C_A, M	$1/\tau_{AB}$, sec^{-1}	$1/\tau_A$, sec^{-1}	C_{AB}/C_A	$(1/\tau_A)/(C_{AB}/C_A)$
0.258	0.384	9.3	7.85	0.672	11.67
0.407	0.099	8.8	...[a]	4.10	...[a]
0.361	0.099	9.4	37.7	3.63	10.4
0.302	0.146	9.1	19.2	2.08	8.2
0.241	0.225	9.4	9.6	1.07	9.0
0.099	0.245	10.7	4.08	0.406	10.1
0.227	0.168	10.7	16.3	1.38	11.8
		Av 9.6			Av 10.37

[a] In this sample the lifetime of $(CH_3)_3Ga$ could not be measured because the resonance line was too broad.

These data can be explained by assuming a dissociation mechanism

$$(CH_3)_3GaN(CH_3)_2H \underset{k_2}{\overset{k_1}{\rightleftharpoons}} (CH_3)_3Ga + N(CH_3)_2H$$

where the rate and lifetime are given by

$$\frac{d[(CH_3)_3Ga]}{dt} = k_1[(CH_3)_3GaN(CH_3)_2H]$$

and

$$1/\tau_{(CH_3)_3Ga} = k_1\frac{[(CH_3)_3GaN(CH_3)_2H]}{[(CH_3)_3Ga]}$$

(4) A. C. Rutenberg, A. A. Palko, and J. S. Drury, *J. Am. Chem. Soc.*, **85**, 2702 (1963); A. C. Rutenberg, A. A. Palko, and J. S. Drury, *J. Phys. Chem.*, **68**, 976 (1964); A. C. Rutenberg and A. A. Palko, *ibid.*, **69** 527 (1965).

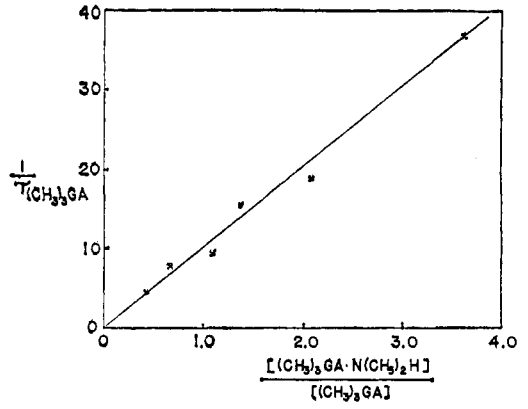

Figure 2. A test of the rate expression $1/\tau_{(CH_3)_3Ga}$ *vs.* the ratio of the concentrations $C_{(CH_3)_3GaN(CH_3)_2H}/C_{(CH_3)_3Ga}$ at +11°. The slope of the line is 10.3 sec^{-1}.

age value obtained from the temperature dependence of τ_A^{-1} and of τ_{AB}^{-1} for which values of 18.9 and 19.4 kcal/mole were obtained.

The resonance for the amine protons in the above solutions consists of a slightly broadened doublet centered at δ −2.37 ppm from TMS with J_{H-CH_3} = 5.4 cps as shown in Figure 4A. Integration of the area under this doublet shows that this resonance corresponds to the six methyl protons of dimethylamine. The CH_3–H coupling was identified by deuteration of the proton attached to the nitrogen. The nmr spectrum of $(CH_3)_3Ga$–$N(CH_3)_2D$ consisted of a single resonance for the methylamine protons at −2.367 ppm and one for the methyl protons on the gallium at 0.695 ppm as shown in Figure 4B. The resonance due to the N–H proton appears to be very broad and centered at approximately δ 3.58 ppm in solutions contain-

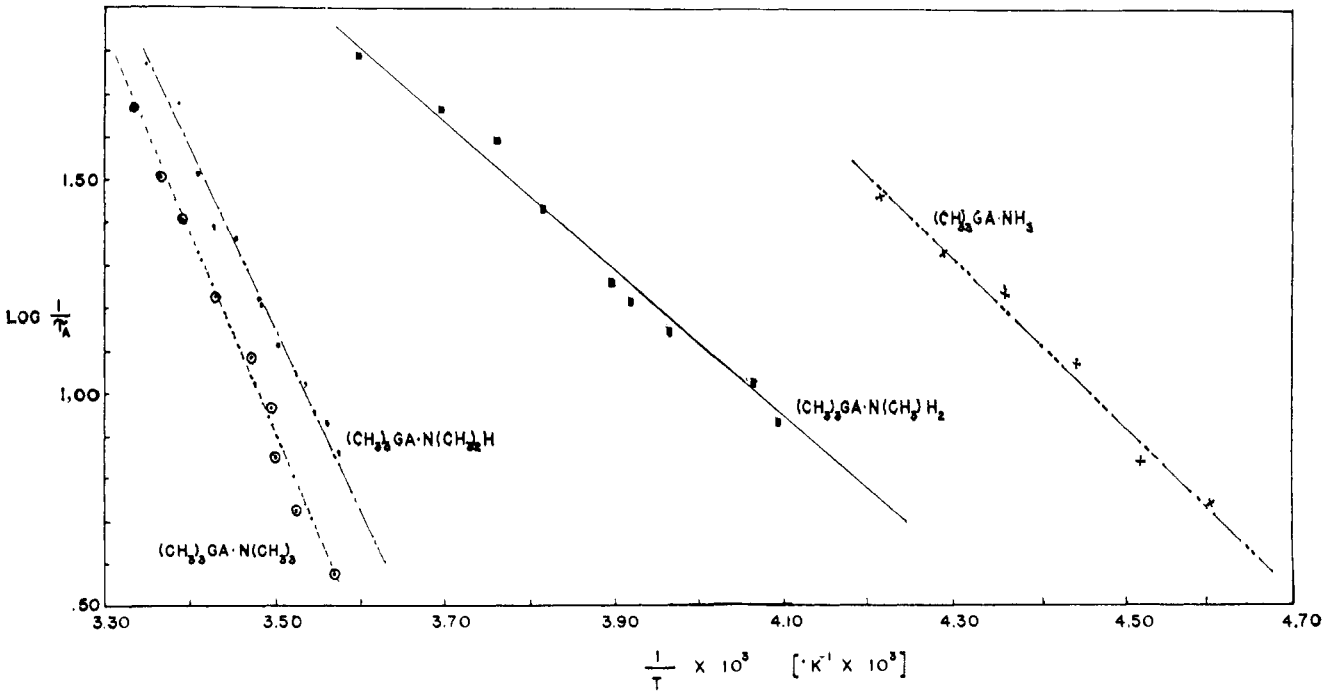

Figure 3. The least-squares plot for the activation energy, log $1/\tau$ *vs.* $1/T$(°K^{-1}): ·····, $(CH_3)_3GaN(CH_3)_3$, $\Delta E^{\ddagger}$ = 23.2 kcal/mole; – – – –, $(CH_3)_3GaN(CH_3)_2H$, $\Delta E^{\ddagger}$ = 19.2 kcal/mole; ———, $(CH_3)_3GaN(CH_3)H_2$, $\Delta E^{\ddagger}$ = 10.4 kcal/mole; – – – –, $(CH_3)_3GaNH_3$, $\Delta E^{\ddagger}$ = 8.5 kcal/mole.

Similarly

$$1/\tau_{(CH_3)_3GaN(CH_3)_2H} = k_1$$

Table I also shows that $1/\tau_{(CH_3)_3GaN(CH_3)_2H}$ = 9.6 sec^{-1} at 11°. Figure 2 shows that a plot $1/\tau_{(CH_3)_3Ga}$ *vs.* $[(CH_3)_3GaN(CH_3)_2H]/[(CH_3)_3Ga]$ is linear with a slope = 10.3 sec^{-1} = k_1.[5] This indicates that the dissociation mechanism is consistent with the observed data. If the exchange process in this system were complicated by a displacement reaction, one should see a concentration dependence for the lifetime of $(CH_3)_3GaN(CH_3)_2H$. The activation energy for the exchange process of 19.2 kcal/mole (Figure 3) lends further support to the dissociation mechanism since the dissociation energy for $(CH_3)_3GaN(CH_3)_2H$ is estimated to be approximately 20 kcal/mole.[6] The value of 19.2 kcal/mole is an aver-

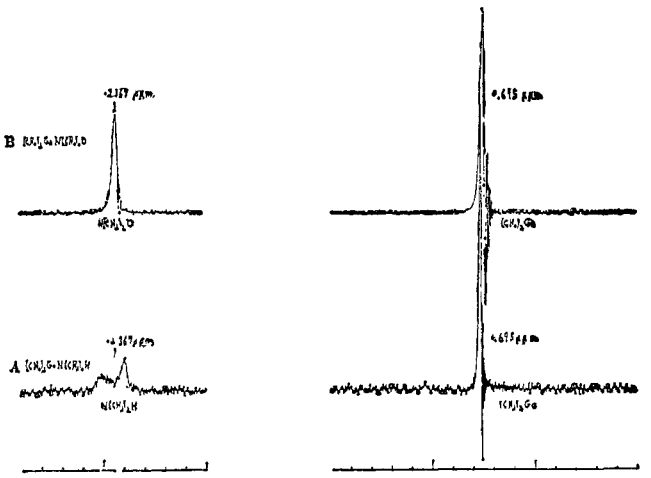

Figure 4. Nmr spectrum at 36°: (A) $(CH_3)_3GaN(CH_3)_2H$; (B) $(CH_3)_3GaN(CH_3)_2D$.

(5) This treatment corresponds to that given in ref 2 by noting that $K_1 = K_e k_2$.

(6) A. Leib, M. T. Emerson, and J. P. Oliver, *Inorg. Chem.*, 4, 1825 (1965).

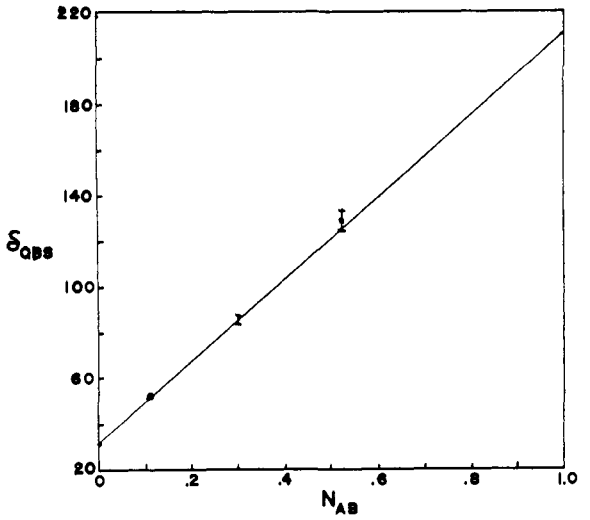

Figure 5. Observed chemical shift of the N-H protons *vs.* mole fraction of $(CH_3)_3GaN(CH_3)H_2$ at 36° (extrapolation to N_{AB} = 1 gives 215 cps).

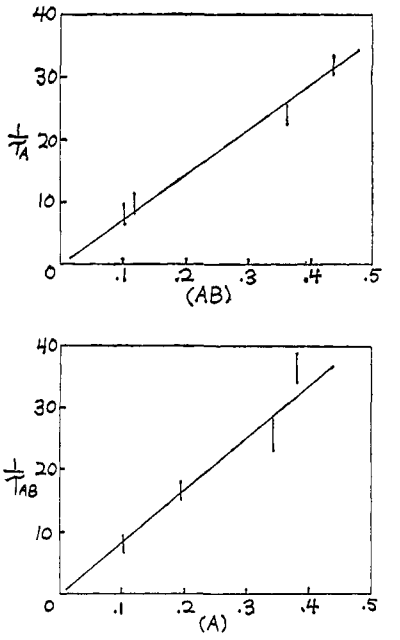

Figure 6. Tests of the bimolecular rate law for the $(CH_3)_3Ga$–$N(CH_3)H_2$ system at −9°; $1/\tau_{(CH_3)_3Ga}$ *vs.* $C_{(CH_3)_3GaN(CH_3)H_2}$ and $1/\tau_{(CH_3)_3GaN(CH_3)H_2}$ *vs.* $C_{(CH_3)_3Ga}$. The slopes of these lines are 73.2 and 81.4 l./mole sec, respectively.

ing the pure addition compound, $(CH_3)_3GaN(CH_3)_2H$, and in solutions containing excess $(CH_3)_3Ga$. In solutions of $(CH_3)_3GaN(CH_3)_2H$, in the presence of excess base, one observes the doublet for the CH_3 protons for small concentrations of base and a singlet for large base concentrations [>2(base):1(acid)]. With an increasing concentration of excess base, a broadened peak emerges from the base line and moves upfield toward the position of the N-H resonance in free $(CH_3)_2NH$. A plot of the mole fraction of $(CH_3)_3$-Ga-$N(CH_3)_2H$ formed in these solutions *vs.* the observed chemical shift of the N-H proton is linear (Figure 5) in the regions where the N-H resonance was narrow enough to observe. This straight line extrapolates to a value of 3.58 ppm for the chemical shift of the N-H proton in the pure adduct. Attempts have been made to observe this resonance, but only a doubtful indication of the resonance could be obtained by integration. It appears that this resonance is broadened due to the N^{14} quadrupole interacting with the asymmetric field surrounding the nitrogen nucleus and N^{14}–H coupling. Attempts to decouple the N^{14} nucleus are in progress.

The $(CH_3)_3Ga$–$N(CH_3)H_2$ System. In this system a linear dependence of the $(CH_3)_3Ga$ resonance with concentration was observed at 36° indicating rapid exchange. This exchange could be slowed giving separate resonance lines for the free and complexed $(CH_3)_3$-Ga at −9°. The lifetimes for both species show a marked concentration dependence as seen in Table II. This clearly shows that a mechanism other than dissociation must provide the predominant path for this exchange process. If one assumes the reaction

$$(CH_3)_3GaN(CH_3)H_2 + (CH_3)_3Ga' \underset{k_1}{\overset{k_1}{\rightleftharpoons}} (CH_3)_3Ga'N(CH_3)H_2 + (CH_3)_3Ga$$

then

$$\frac{d[(CH_3)_3GaN(CH_3)H_2]}{dt} = k_1[(CH_3)_3GaN(CH_3)H_2] \times [(CH_3)_3Ga]$$

and by definition

$$\frac{[(CH_3)_3GaN(CH_3)H_2]}{\tau_{(CH_3)_3GaN(CH_3)H_2}} = \frac{d[(CH_3)_3GaN(CH_3)H_2]}{dt}$$

It follows that

$$\frac{1}{\tau_{(CH_3)_3GaN(CH_3)H_2}} = k_1[(CH_3)_3Ga]$$

and similarly

$$\frac{1}{\tau_{(CH_3)_3Ga}} = k_1[(CH_3)_3GaN(CH_3)H_2]$$

Thus the lifetimes of $(CH_3)_3GaN(CH_3)H_2$ (τ_{AB}) and $(CH_3)_3Ga$ (τ_A) are both directly related to the molar concentrations of Lewis acid and adduct in the solution. Figure 6 shows plots of τ_{AB}^{-1} *vs.* C_A and τ_A^{-1} *vs.* C_{AB} which are linear and pass through the origin with an average slope of 77.3 l./mole sec. The activation energy for this exchange process is 10.4 kcal/mole which is approximately one-half the dissociation energy of the $(CH_3)_3GaN(CH_3)H_2$ adduct, indicating a low-energy displacement pathway for this exchange. Any contribution to the rate of reaction from the dissociation mechanism must be very small since this would increase the slope of the Arrhenius plot with increasing temperature. Figure 3 shows that $\Delta E^{\pm}$ is constant over the temperature range studied.

Table II. Concentration Dependence of the Lifetimes of $(CH_3)_3GaN(CH_3)H_2$ (τ_{AB}) and $(CH_3)_3Ga$ (τ_A) at −9°

C_{AB}, *M*	C_A, *M*	$1/\tau_{AB}$, sec^{-1}	$1/\tau_A$, sec^{-1}
0.364	0.344	25.45	24.19
0.436	0.103	7.70	(32.25)[a]
0.0997	0.379	(37.00)[a]	8.80
0.118	0.195	(16.93)[a]	9.74

[a] These τ^{-1} are estimated from resonance lines which are too broad to satisfy the conditions of slow exchange by calculation of theoretical line shapes.

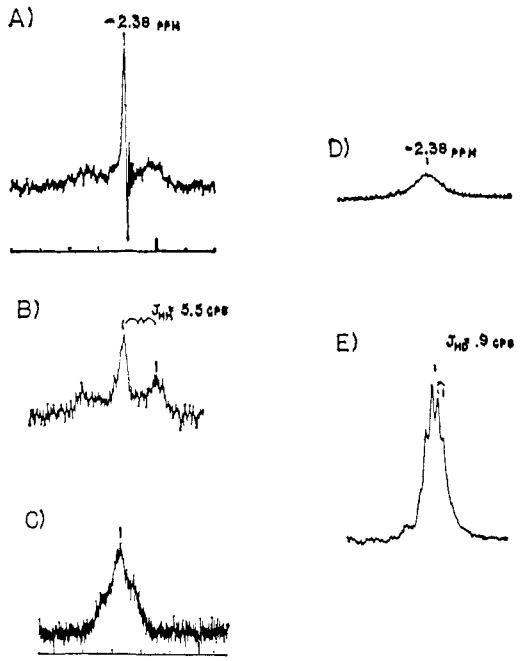

Figure 7. Nmr resonance spectra of the amine protons of $(CH_3)_3GaN(CH_3)H_2$ in Freon 11: (A) $(CH_3)NH_2$ resonance in solution where $C_{(CH_3)_3Ga} > C_{(CH_3)NH_2}$. (B) $(CH_3)NH_2$ resonance in solutions where $C_{(CH_3)_3Ga} < C_{N(CH_3)H_2}$; (C) $(CH_3)NH_2$ resonance in solutions where $C_{(CH_3)_3Ga} \ll C_{N(CH_3)_3H_2}$; (D) $(CH_3)NH_2$ resonance in a solution of $(CH_3)_3GaN(CH_3)H_2$ in which the concentration is greater than 1 N; (E) $(CH_3)ND_2$ resonance in $(CH_3)_3GaN(CH_3)D_2$ showing J_{HD} = 0.9 cps.

The nmr resonance for the amine protons in $(CH_3)_3GaN(CH_3)H_2$ consists of three peaks centered at −2.40 ppm below TMS. In the presence of excess $(CH_3)_3Ga$ the middle peak of the these three sharpens and integration of the area under all three peaks indicates that these represent all of the protons on CH_3NH_2 (Figure 7A). In a concentrated sample of pure $(CH_3)_3GaN(CH_3)H_2$, the resonance for the amine protons is a very broad line centered at −2.40 ppm, and again the area under the peak integrates for all of the amine protons (Figure 7D). In the presence of excess monomethylamine, the nmr absorption shows a broadened triplet (J_{HNCH} = 5.6 cps) with an area which integrates for only the methyl protons on $(CH_3)NH_2$ (Figure 7B).

The fact that the NH resonance is not readily observable under these conditions is probably due to two factors. The first of these is N^{14}–H^1 coupling which is of the order of 50 cps.[7] This would give rise to a triplet structure with only one-third of the intensity of the proton located at the predicted position. The second is that the N^{14} quadrupole moment will give rise to additional line broadening of the proton spectrum since the field around it is not completely symmetrical. In samples with a large excess of $(CH_3)NH_2$ ($N_{AB} < 0.3$) one observes a broadened resonance due to the N–H protons. A plot of the observed chemical shift of the N–H protons *vs.* the mole fraction of base appears to be linear over the very limited concentration range where the N–H resonance is observable ($N_{AB} < 0.3$). Extrapolation of this line to $N_{AB} = 1$ shows that the resonance for the N–H proton should be at −1.78 ppm; however, no visible resonance could be found at this position.

(7) M. T. Emerson, E. Grunwald, M. L. Kaplan, and R. A. Kromhout, *J. Am. Chem. Soc.*, **82**, 6307 (1960).

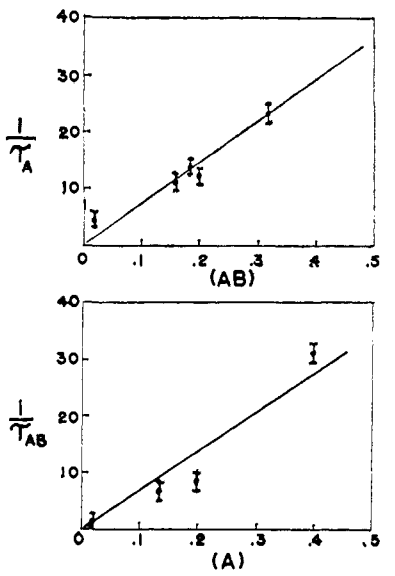

Figure 8. Tests of the rate law for the $(CH_3)_3Ga$–NH_3 system at −40°: $1/\tau_{(CH_3)_3Ga}$ *vs.* $C_{(CH_3)_3GaNH_3}$ and $1/\tau_{(CH_3)_3GaNH_3}$ *vs.* $C_{(CH_3)_3Ga}$: The slopes of these lines are 67.5 l./mole sec.

Some evidence for this interpretation is provided by taking the spectrum of $(CH_3)_3GaN(CH_3)D_2$, which consists of a single line at 0.60 ppm, the methylgallium protons, and a closely spaced multiplet (J_{HD} = 0.9 cps) for the methylamine resonance at −2.40 ppm, as shown in Figure 7E. This multiplet structure for the amine resonance is due to the deuterium coupling with the methylamine protons, J_{D-H} = 0.9 cps, giving the expected lines for interaction of two spins of I = 1 with spins of I = $^1/_2$. The order of the magnitude of this coupling is approximately that which is predicted (about one-sixth of the proton–proton coupling) from other methyl–ammonium systems.[7]

The $(CH_3)_3Ga$–NH_3 System: Rapid exchange with excess $(CH_3)_3Ga$ is again shown by observing the linear dependence for the chemical shift of the $(CH_3)_3Ga$ protons on the mole fraction of either free acid or complex. The lifetimes of $(CH_3)_3Ga$ (τ_A) and $(CH_3)_3GaNH_3$ (τ_{AB}) are again found to be concentration dependent as shown in Table III.

Table III. Concentration Dependence of the Lifetimes of $(CH_3)_3Ga$ (τ_A) and $(CH_3)_3GaNH_3$ (τ_{AB}) at −40°

		$1/\tau$, sec^{-1}	
C_A, M	C_{AB}, M	A	AB
1.056	0.197	11.31	(64.60)[a]
0.395	0.186	14.77	31.10
0.198	0.158	12.25	7.85
0.012	0.31	...[b]	1.88
0.132	0.07	3.2	6.60

[a] Resonance lines were too broad to measure half-widths accurately but were calculated from theoretical line shapes. [b] Too broad to be estimated.

If again one assumes a bimolecular displacement (eq 2) for the exchange, then

$$1/\tau_{(CH_3)_3Ga} = k_1[(CH_3)_3GaNH_3]$$

and

$$1/\tau_{(CH_3)_3GaNH_3} = k_1[(CH_3)_3Ga]$$

Figure 8 shows that the plots of $^1/\tau_A$ *vs.* C_{AB} and $1/\tau_{AB}$ *vs.* C_A are linear with an average slope of 67.5 l./mole sec.

Table IV. Change in Chemical Shift with Temperature in the $(CH_3)_3Ga$–$O(CH_3)_2$ System[a]

C_A, M	C_B, M	36° AB	36° BA	−40° AB	−40° BA	−100° AB	−100° BA
0.59	0.68	1.971	−1.825	2.013	−1.841		
0.465	0.346	1.864	−1.859	1.902	−1.881		
0.841	0.128	1.572	−1.861	1.591	−1.880	1.601	−1.881
0.163	0.799	1.974	−1.710	2.001	−1.718	2.048	−1.725
K_e (25°)		K_e (−40°)					
3.73×10^{-2}		8.48×10^{-3}					
1.17×10^{-2}		1.27×10^{-3}					
6.59×10^{-2}		...					
4.55×10^{-2}		2.7×10^{-3}					

[a] Chemical shifts in ppm from C_5H_{10}.

Furthermore, the activation energy for this exchange is 8.5 kcal/mole which is much lower than the estimated heat of dissociation of the adduct (20 kcal/mole). Since there is no observable change in slope of the activation energy plot, we can assume there is very little contribution to the rate laws from a dissociation mechanism.

The appearance of the nmr spectrum of the N–H protons in this system depends upon the relative concentrations of $(CH_3)_3Ga$ and NH_3. When excess $(CH_3)_3Ga$ is present a very broad resonance (≈200 cps wide) is observed upon integration of the spectrum. This is centered near δ −1.3 ppm, but no accurate value can be given for the chemical shift. When a large excess (6.16:1 NH_3:$(CH_3)_3Ga$) of NH_3 is present, a well-defined but broadened triplet appears with $J_{N^{14}-H} \approx 60$ cps. This coupling is in good agreement with the values observed in the NH_4^+ ion ($J_{N^{14}-H} = 54.3$ cps).[7]

The majority of the line broadening is certainly due to the N^{14}–H coupling and to the N^{14} quadrupole moment when excess $(CH_3)_3Ga$ is present. Exchange broadening may also be present but this cannot be detected. With excess NH_3 present residual quadrupole effects will cause broadening, but exchange effects may be of more importance. Definitive experiments have not yet been performed to distinguish these effects.

The $(CH_3)_3Ga$–$O(CH_3)_2$ System. This system has also been shown to undergo rapid exchange as evidenced by the occurrence of a single resonance line for the $(CH_3)_3Ga$ and a single line for the $O(CH_3)_2$ protons which are concentration dependent. This was found to be true even at −100° where the resonance lines for $(CH_3)_3Ga$ and $O(CH_3)_2$ protons were narrower than that for cyclopentane which was used as an internal standard. A plot of mole fraction calculated on the basis of complete adduct formation *vs.* the chemical shift observed at room temperature is not linear as seen in Figure 9. This can readily be interpreted on the basis of the equilibrium

$$(CH_3)_3GaO(CH_3)_2 \rightleftharpoons (CH_3)_3Ga + O(CH_3)_2 \qquad (4)$$

where the chemical shift is dependent on the total concentration of each species present.

Nmr spectra of samples of varying concentration of acid and base were run at −40 and −100°, which showed a change in chemical shift of the gallium protons and the dimethyl ether protons with temperature (Table IV). If one assumes that chemical shift values observed at −100°, $\delta_{(CH_3)_3GaO(CH_3)_2}$ 2.047 and $\delta_{(CH_3)_3GaO(CH_3)_2}$ −1.881 ppm, are for the undissociated adduct, then the equilibrium constants for reaction 4 may be calculated at 25 and −40° from the observed chemical shifts given by

$$\delta^{obsd}{}_{(CH_3)_3Ga} = (N_{(CH_3)_3Ga})(\delta^0{}_{(CH_3)_3Ga}) + (N_{(CH_3)_3GaO(CH_3)_2}) \times (\delta_{(CH_3)_3GaO(CH_3)_2})$$

and

$$\delta^{obsd}{}_{O(CH_3)_2} = (N_{O(CH_3)_2}(\delta^0{}_{O(CH_3)_2}) + (N_{(CH_3)_3GaO(CH_3)_2}) \times (\delta^0{}_{(CH_3)_3GaO(CH_3)_2})$$

The following equation also holds

$$C_{(CH_3)_3Ga} = C^0{}_{(CH_3)_3Ga} - C_{(CH_3)_3GaO(CH_3)_2}$$

Thus, given the initial concentration and the chemical shift data one can calculate the concentrations in a system under any conditions and evaluate the equi-

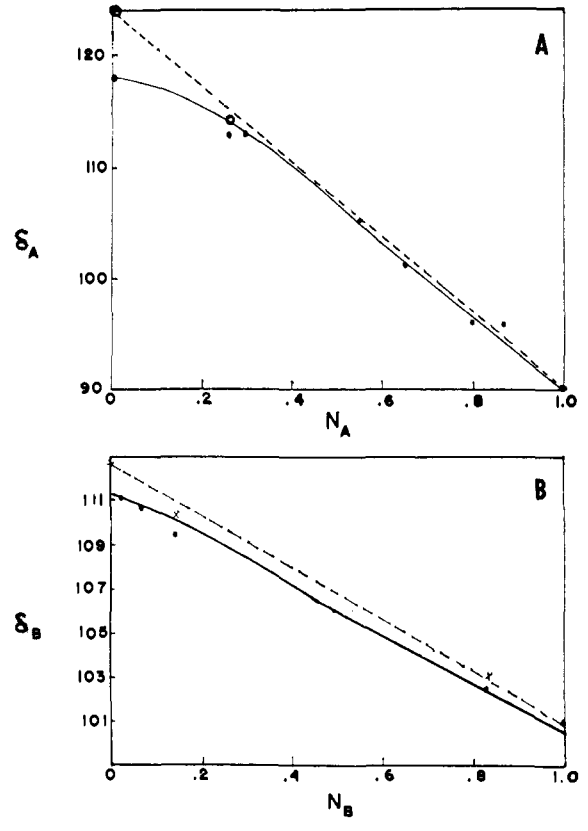

Figure 9. Plot of observed chemical shifts for $(CH_3)_2O$ and $(CH_3)_3Ga$ *vs.* mole fraction assuming all possible adduct is formed. (A) Plot of δ^{obsd} *vs.* $N_{(CH_3)_3Ga}$ at 36° (- - - -) and δ^{obsd} *vs.* $N_{(CH_3)_3Ga}$ at −100° (———). (B) Plot of δ^{obsd} *vs.* $N_{(CH_3)_2O}$ at 36° (- - - -) and δ^{obsd} *vs.* $N_{(CH_3)_2O}$ at −100° (———).

Table V. Summary of Nmr Data and Activation Energies for Some $(CH_3)_3Ga$ Systems

	CH_3-Ga, ppm	N-CH_3, ppm	N-H, ppm	J_{H-NCH_3}, cps	$-\Delta E^{\ddagger}$, kcal/mole — a	— b	$\Delta S^{\ddagger}$, eu[c]	ΔH_{dis}, kcal/mole
$(CH_3)_3GaN(CH_3)_3$	0.666	−2.292	...	...	25.3[d]	22.3[d]	29.76	21[e]
$(CH_3)_3GaN(CH_3)_2H$	0.662	−2.383	...	5.4	19.4	18.9	12.35	21[f]
$(CH_3)_3GaN(CH_3)H_2$	0.594	−2.38	...	(5.6)	11.6	8.2	−13.21	17[f]
$(CH_3)_3GaNH_3$	0.630	...	...	...	8.0	8.9	−15.10	18.5[f]
$(CH_3)_3GaO(CH_3)_2$	0.552	−3.376	...	...	<10	<10		9[e]
$(CH_3)_3Ga$	0.0	...	...	...	...	...	...	...
$(CH_3)_3N$	...	−2.084	...	...	...	...	...	...
$(CH_3)_2NH$	...	−2.317	−0.30	...	...	...	...	...
$(CH_3)NH_2$	...	−2.367	−0.70	...	...	...	...	...
NH_3	...	...	−0.458	...	...	...	...	...
$O(CH_3)_2$	...	−3.173	...	...	...	...	...	...

[a] Calculated from the temperature dependence of τ_{AB}^{-1} by a least-squares procedure. [b] Calculated from the temperature dependence of τ_A^{-1} by a least-squares procedure. [c] $\Delta S^{\ddagger}$ was calculated by the procedure given in S. Glasstone, K. Laidler, and H. Eyring, "The Theory of Rate Processes," McGraw-Hill Book Co., Inc., New York, N. Y., 1941, p 197. [d] Reference 2. [e] Reference 8. [f] Estimated from observed δ_A from ref 6.

librium constant. The results of these calculations are given in Table IV.

These data indicate that the equilibrium constant is a weak function of temperature which is predicted by the low (10 kcal/mole) dissociation energy[8] for this

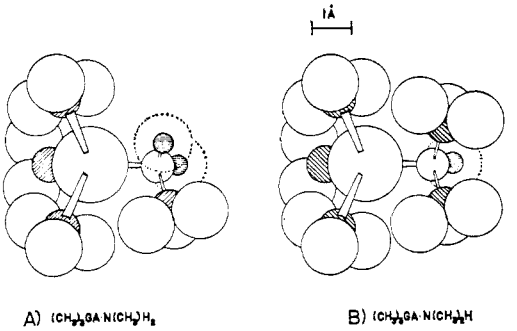

Figure 10. (A) $(CH_3)_3GaN(CH_3)H_2$ assuming tetrahedral symmetry of the gallium and nitrogen atoms shown with van der Waals radii for all protons. (B) $(CH_3)_3GaN(CH_3)_2H$ assuming tetrahedral symmetry of the gallium and nitrogen atoms shown with van der Waals radii for all protons.

adduct. It is impossible to obtain kinetic parameters for this reaction since no line broadening can be observed with the instrumentation available (−100°). This does, however, allow an upper limit to be set for the lifetime of $(CH_3)_3GaO(CH_3)_2$, $(CH_3)_3Ga$, and $O(CH_3)_2$ of 10^{-3} sec and a maximum of 10 kcal/mole to be estimated for the activation energy.

Discussion

The mechanisms of exchange reactions involving trimethylgallium–amine adducts in the presence of excess $(CH_3)_3Ga$ show a remarkable sensitivity to the structure of the base. The exchange reactions involving $(CH_3)_3GaN(CH_3)_3$ and $(CH_3)_3GaN(CH_3)_2H$ clearly proceed by a dissociation mechanism as can be seen by the concentration independence of the lifetimes of the adduct molecules and the high activation energy for the exchange summarized in Figure 3 and Table V.

The path for exchange goes abruptly from this route to the displacement path (eq 2), as evidenced by the same parameters for the $(CH_3)_3Ga$–$N(CH_3)H_2$ and $(CH_3)_3Ga$–NH_3 systems. This change can be explained by examining the ability of the "large" $(CH_3)_3Ga$ molecules to attack the amine portion of the $(CH_3)_3Ga$–NR_3 adduct. For $(CH_3)_3GaN(CH_3)_3$ and $(CH_3)_3GaN(CH_3)_2H$, a consideration of molecular models shows that these amines are well protected from electrophilic attack of the "large" $(CH_3)_3Ga$ molecules by the methyl groups surrounding the nitrogen (Figure 10B). Therefore, exchange of $(CH_3)_3Ga$ can only occur after the adduct has dissociated. In the case of $(CH_3)_3GaNH_2(CH_3)$ and $(CH_3)_3GaNH_3$, molecular models show that the amine portion of the adduct is now open to electrophilic attack by the $(CH_3)_3Ga$ (Figure 10A). This then allows the bimolecular transition state to be stabilized so that exchange may proceed by a low-energy displacement reaction. This is seen clearly in the drop in activation energy to 10 kcal/mole for these systems and a change in the entropy of activation.

In the $(CH_3)_3Ga$–$O(CH_3)_2$ system the rate of exchange of acid and base molecules is so rapid that the nmr spectrum appears as two single sharp lines even at −100°. Since the dissociation energy of the $(CH_3)_3Ga$–$O(CH_3)_2$ adduct is 10 kcal/mole, one would predict that, if the exchange reaction proceeds by a dissociation process, line broadening would be observed in the same temperature region for the $(CH_3)_3Ga$–NH_3 system (−30 to −50°) since the activation energy for this exchange is 8 kcal/mole. One thus may conclude that because no line broadening is observed even at −100° the mechanism for this exchange is an electrophilic displacement similar to the $(CH_3)_3Ga$–$N(CH_3)H_2$ and $(CH_3)_3Ga$–NH_3 systems. This is in accord with the previous arguments since $O(CH_3)_2$ is not sterically hindered and even provides an extra electron pair for adduct bond formation in the transition state.

If the same arguments are applied to the BF_3–ether systems, one would predict that exchange with excess BF_3 should take place by either pathway 1 or 2. For small unsterically hindered ethers, BF_3 could easily attack the electron pair on the ether giving a low-energy pathway for exchange. However, in BF_3–trialkylamine systems the BF_3 could not attack the protected amine and exchange could only occur after dissociation. This is indeed what is observed for the BF_3–$N(CH_2CH_3)_3$ system where Brownstein, *et al.*,[3] observed no effective exchange by F^{19} line broadening while very rapid exchange and low activation energies

(8) G. E. Coates, *J. Chem. Soc.*, 2003 (1951).

were observed for the BF_3–OR_2 systems.[3,4] The only exception to this type of analysis is the BF_3–pyridine system which appears to undergo very rapid exchange with a low activation energy even though its dissociation energy is high. This, however, fits the proposed arguments when one realizes that pyridine is flat and the nitrogen is open to attack.

In conclusion it appears that the exchange reaction in the Lewis acid–base systems examined so far in this laboratory proceed rapidly by either a dissociation or a displacement reaction in the presence of excess Lewis acid depending upon the ability of this acid molecule to attack the base present in the addition compound. This explanation also appears to apply to the exchange reaction in BF_3–Lewis base systems. It should be further pointed out that when the ΔH_{dis} approaches the energy of activation for the substitution reaction both processes may be present leading to a *complex reaction*. This appears to be the case in several of the BF_3–base systems which have been reported.[4]

The mechanism for exchange in the systems where "all" material is complexed is not yet clear since in the only systems studied so far, insufficient information has been presented to delineate all possible pathways. It is clear, however, that in these cases a more complex mechanism such as

$$AB \longrightarrow A + B$$

followed by

$$A + A'B' \longrightarrow AB' + A'$$

could result with all of the consequences of the chain mechanism. This path is suggested as an alternate to (3) previously proposed. Further complications are found in these reactions when extending the investigation to systems having excess base. In the $(CH_3)_3Ga$ systems so far studied, the reactions all proceed very rapidly as evidenced by the fact that only one type of base can be observed even at $-100°$. On this basis it is possible to rule out a dissociation path since this has been established to proceed at readily measurable rates.

This rapid exchange may be rationalized by noting that the $(CH_3)_3Ga$ in the adduct is not sterically hindered (Figure 10) and is therefore amenable to attack by the nucleophile, NR_3 or OR_2. Further this is compatible with the fact that diadducts of boron derivatives have been observed at low temperature[9] and should be possible for the gallium compounds where d orbitals are also available for bond formation. Thus, the displacement path appears to provide an attractive low-energy route for base exchange which is in accord with the experimental data. It is unfortunate that definitive experiments cannot be performed by the line-broadening techniques currently available in this laboratory.

Additional observations have been made on the base portion of these addition compounds which require comment. Figures 4 and 7 show the nmr spectra of the $N(CH_3)_2H$ and $N(CH_3)H_2$ systems under various conditions, and it is quite clear that more complex coupling is present in the addition compounds than in the free bases. In the $(CH_3)_3Ga$–$N(CH_3)_2H$ system with excess $(CH_3)_3Ga$, proton–proton coupling occurs across the C–N linkage (Figure 4a, $J_{H-H} = 5.4$ cps). Proof of this was obtained by deuteration of the N–H proton which caused collapse of the doublet (Figure 4B). This type of coupling was also present in the $(CH_3)_3Ga$–$N(CH_3)H_2$ system under the same conditions (Figure 7A). On deuteration this triplet collapsed into a closely spaced multiplet in which H–D coupling ($J_{H-D} = 0.9$ cps) was indicated (Figure 7E). The magnitude of these coupling constants is similar to that reported in the $N(CH_3)H_3^+$ ion.[10] N^{14} coupling with the protons directly attached to the nitrogen also appears to be present in all cases with $J_{N^{14}-H} = 60$ cps, which is similar to other $N^{14}H^1$ coupling constants.[7] It is difficult to observe this interaction in most instances because the lines are badly broadened by quadrupole relaxation effects arising from the lack of complete symmetry surrounding the N^{14} nucleus. This is also in accord with the lack of N^{14}–CH_3 coupling since the N^{14} relaxation is fast compared to the N^{14}–CH_3 spin–spin interaction.[10,11]

Another interesting observation which has been made is that the proton–proton coupling and N^{14}–H^1 coupling in the base do not disappear when small excess concentrations of base are present, even though rapid exchange of bases has been proven.[2] The most pronounced case of this is in fact in the NH_3 system where N^{14}–H^1 coupling persists when a 6:1 excess in base is present. The couplings disappear at lower base:acid ratios for the other systems. This phenomenon is of interest since it implies that the spin–spin coupling does not collapse at the same rate as the chemical shift. Several possible explanations for this behavior might be made, but none gives a completely satisfactory treatment of all the available data. Further work is now under way to elucidate this phenomenon and to determine the mechanism of base exchange.

(9) H. C. Brown, P. F. Stehle, and P. A. Tierney, *J. Am. Chem. Soc.*, **79**, 2020 (1957).

(10) E. Grunwald, A. Loewenstein, and S. Meiboom, *J. Chem. Phys.*, **27**, 630 (1957).

(11) H. S. Gutowsky, D. McCall, and C. P. Slichter, *ibid.*, **21**, 279 (1953).